International Journal of Recent Engineering Research and Development (IJRERD)
ISSN: 2455-8761
www.ijrerd.com || Volume 08 – Issue 03 || March 2023 || PP. 01-15

Influence of brace slenderness ratio on seismic performance of frame-brace structure

Yang Xinyu[1], LIN Yongle[2],

[1,2]Henan Polytechnic University，School of Civil Engineering
Jiaozuo city, Henan province, China

Abstract: In order to study the impact of brace slenderness ratio on the seismic performance of frame-braced structural systems, the finite element models of eccentrically braced and centrally braced steel frames were established using ABAQUS/Standard analysis method based on pseudo-static tests of eccentrically braced steel frames. The seismic performance of the two structures under different slenderness ratios was analyzed. The results show that the seismic resistance of frames with a small slenderness ratio of braces is generally better, and the change in slenderness ratio has a more significant impact on the seismic resistance of central braced structures; The gradual decrease in the slenderness ratio of the brace has a negligible impact on the ultimate bearing capacity, hysteretic performance, and energy consumption of eccentrically braced structures. However, a significant impact on ductility and initial stiffness will accelerate the degradation rate of the initial stiffness of the structure. A decrease in the brace slenderness ratio of a centrally braceed structure will increase the ultimate bearing capacity, hysteretic performance, initial stiffness, and ductility of the structure, with a ratio of 1:1 between the slenderness ratio reduction rate and the initial stiffness increase rate; However, if the slenderness ratio is too small, it will lead to excessive brace, leading to early failure of beams and columns. Considering the structure's material properties and seismic performance, it recommended taking $61.61<\lambda<100$.

Keywords: slenderness ratio; frame-braced structure; Stress characteristics; seismic performance

1. Introduction

Inclined braces are installed between pure steel frame columns to form an effective anti-lateral displacement structure, namely, a frame-brace structure system. Brace and framework cooperatively to effectively improve the lateral stiffness of the structure and thereby control the structure's lateral deformation, which can divide into two types: central brace and eccentric brace. The former dissipates energy by setting diagonal braces to make it buckle, allowing the structure to have greater lateral stiffness and bearing capacity; The latter consumes seismic energy by subjecting the energy-dissipating beam segment to shear buckling prior to the same beam segment. Although the failure mechanisms of the two structural systems are different, braces are important load-bearing components, and their slenderness ratio impacts the structure's seismic performance.

Lou Yu studied the seismic performance of steel frame K-shaped braced structures through pseudo-static tests and found that diagonal braces, vertical rods, and beams and columns yield in turn. Among them, diagonal braces are the main energy dissipation components, which can improve the structure's seismic performance[1]. Yang Junfang conducted static pushover tests and numerical simulations to study the seismic performance of centrally braced steel frames. The results show that compression buckling of braces can reduce the lateral stiffness of the structure. However, the decrease in horizontal bearing capacity is insignificant, and the structure still has

good ductility[2]. Sun Yuezhou studied the impact of the brace slenderness ratio limit on the mechanical performance of the structure. They found that increasing the brace slenderness ratio under the same cross-sectional area can improve the brace's fatigue life and reduce the structure's interlayer deformation[3]. CuiYao, through pseudo-static tests of centrally braced frames with different beam-column connections, found that when the column stiffness is weak, the brace cannot fully play its role, resulting in a decrease in the lateral stiffness of the structure; When box columns used, the joint plates at the column ends are prone to local damage and the horizontal bearing capacity reduced[4]. Tremblay conducted hysteretic performance tests on 76 steel brace specimens, respectively studying the effects of specimen width-thickness ratio, end restraint, and slenderness ratio on the hysteretic performance of the center brace[5]. Jouneghani analyzed the seismic performance of elliptically braced frames through pseudo-static tests and numerical simulations. The tests show that elliptically braced frames exhibit good hysteretic performance, strength, ductility, and energy dissipation[6]. Mohammed analyzed the impact of semi-rigid beam-to-column connections on the performance of frames after buckling through numerical simulation and found that compared to unbraced frames, the load-displacement curve of braceed frames is less affected by the stiffness of beam-to-column connections[7]. Rai proposed that during brace design, it is necessary to control the width-thickness ratio limit and amplify the slenderness ratio limit so that the local buckling of the brace does not precede the overall buckling, to avoid premature failure of beams and columns caused by excessive brace[8]. Other scholars and specifications[9]-[17]have also provided suggestions on the limit value of the brace slenderness ratio.

Based on comparative tests, this paper analyzes a series of models using the same finite element method to study the effect of the slenderness ratio of braces on the mechanical properties of steel frames in different structural systems.

2. Test

2.1 Specimen design

The research group completed a 1:2 scale K-type eccentrically braced steel frame quasi-static test[18]. The span between the columns is 3000 mm, the height is 1800 mm, and the length of the energy-consuming beam section is 600 mm. All the members are hot-rolled H-type, and the section size of the members show in table.1. The weld connection is used at each node of the specimen, as shown in Figure.1.

Tab.1 Section size and material

Component type	Section size/mm	Material
Column	HW200×200×8×12	Q345B
Beam	HN250×125×6×9	Q345B
Brace	HN250×125×6×9	Q235B
Energy dissipation beam	HW125×125×6.5×9	Q235B

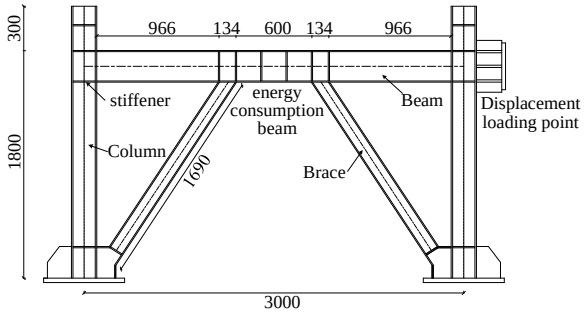

Fig.1 Dimension of specimens (unit: mm)

2.2 Loading process

At the initial stage of the test, an axial load of 200kN was applied to the column top, and then a horizontal reciprocating load was applied to the beam end, as shown in Figure.2.

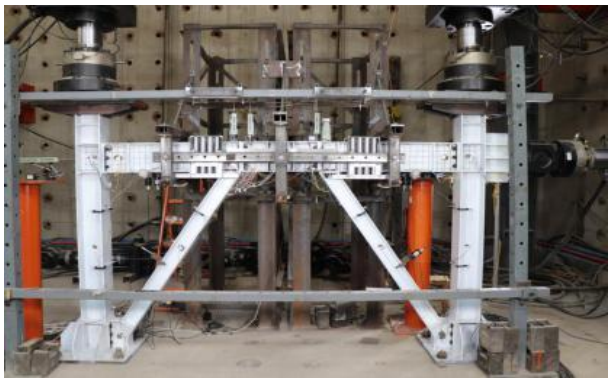

Fig. 2 Loading device

According to the test standard[19], the load-displacement mixed loading system is adopted. Firstly, cyclic loading is started by load control, which is increased step by step until the yield strain occurs. The yield displacement is Δ_y, and the yield force is F_y. Converting into displacement control, an integer multiple of Δ_y gradually increases the load. Each stage is cycled three times until the load drops to 85% of the maximum bearing capacity or the specimen fails to stop the test. The loading system is shown in Figure.3.

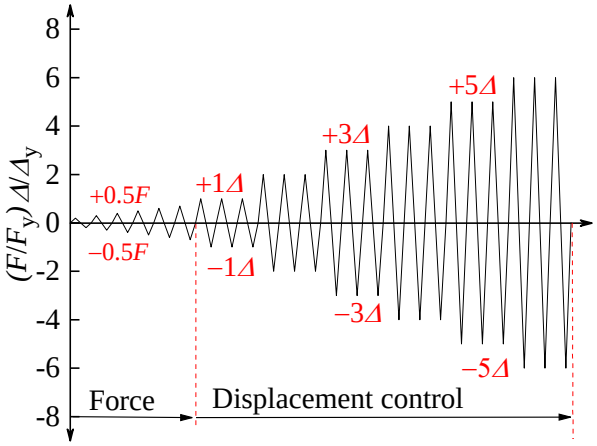

Fig. 3 Loading system

2.3 Test results

Test load to Δ_1, the lower flange at the left end of the energy dissipation beam yielded first, and no significant changes were found in the overall frame. No Δ_5, Δ_6, Δ_7, the flange web of the energy dissipation beam has successively buckled and gradually intensified. Stay Δ The upper part of the 8th stage web is torn Δ. The crack pulled out from the original upper end of the Level 9 web continued to expand, while a crack was also torn out in the middle of the web. After the test, the component damage is shown in Figure.4.

Fig. 4 Failure mode

3. Finite element analysis

3.1 Model Design Overview

By changing the slenderness ratio of the frame brace system and braces, a series of finite element models were established to study the impact of braces on the seismic performance of steel frames, as shown in Table.2. In order to ensure the accuracy of the analysis and reduce the error of comparison, except for the change in the size of the brace section, the dimensions of other components should be consistent with the structural span.

Tab. 2 Material properties of steel

Model Number	Brace	Slenderness ratio
EBF-60	60×3.0	69.57
EBF-80	80×4.0	52.48
EBF-100	100×5.0	41.85
EBF-125	125×125×6.5×9	30.04
CBF-40	40×2.0	109.70
CBF-60	60×3.0	73.16
CBF-70	70×3.5	62.83
CBF-80	80×4.0	55.05
CBF-100	100×5.0	44.01

EBF-Eccentrically beace frame CBF-Center brace frame

3.2 Material Constitutive and Boundary Conditions

The material properties of steel in the finite element model are based on the results of the actual stress-strain parameters of steel measured by the material property test [20]. The results are shown in Table.3. In the analysis process, the model follows the Mises yield criterion, adopts a multilinear follow-up hardening (KINH) material constitutive model, and considers the Bauschinger effect. The model components are all built using shell elements (S4R), and mesh refinement is performed in the node region; The connection between component nodes mainly adopts the Tie method; According to the direction of the three-dimensional coordinate axis, limiting the out-of-plane instability of the entire frame beam with U3=0, The column base adopts rational consolidation to constrain six degrees of freedom; Apply axial force on the top of the columns on both sides in a coupling manner, and apply a leveling force at the position where the column surface is flush with the upper and lower flanges of the beam, as shown in Figure.5.

Tab. 3 Steel material properties

Component	h/mm	f_y/MPa	f_u/MPa	E/GPa	δ/%
Beam	6	367	533.5	210	24.4
	9	352.3	531	210	25.5
Column	8	346	543.5	219	25.1
	12	341.7	530	220	28.8
Beam	6	361.6	453	211	31.6
	9	286	457.6	207	26.2
Energy dissipation beam	6.5	270	445	206	33.4
	9	273.8	440.6	210	31.2

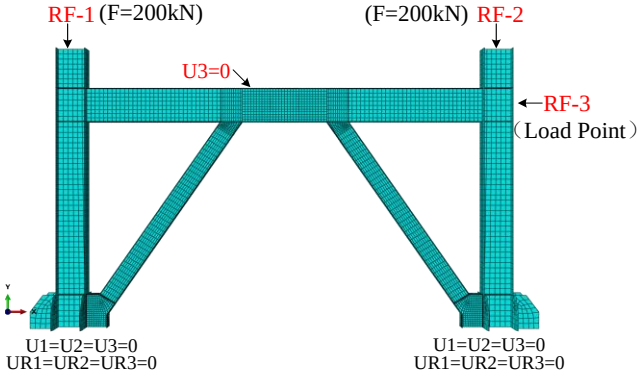

(a) Eccentrically beace frame

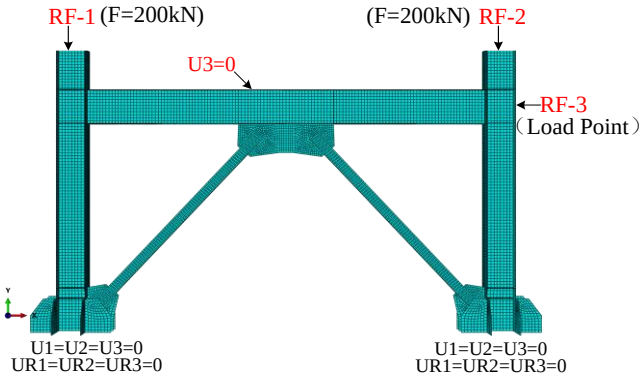

(b) Center brace frame

Fig. 5 Finite element model

3.3 Comparative finite element analysis

Figure.6 and Figure.7 show the hysteretic and skeleton curves obtained from the experimental BASE and finite element EBF-125 model analysis, respectively. The two curves are consistent. The main reason for the difference between the two is that adopting limit measures in the test cannot eliminate the phenomenon of out-of-plane displacement but can completely limit the out-of-plane lateral displacement of the structure in the finite element analysis; The test component has initial defects that cannot fully guarantee the uniformity of the material, and the material properties of the finite element model do not consider initial defects; During the test loading process, there is a certain sliding phenomenon at the column base, and the bottom of the column base in the finite element model can be fully consolidated. The final failure pattern is shown in Figure8, which is consistent with the test and is a shear failure.

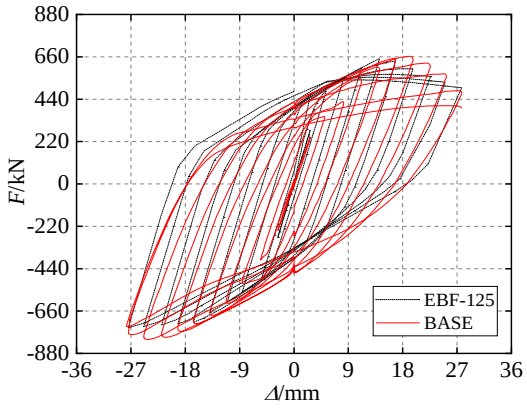

Fig. 6 Hysteresis curve comparison

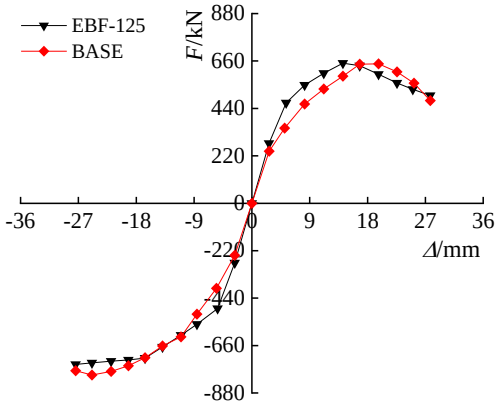

Fig. 7 Skeleton curve comparison

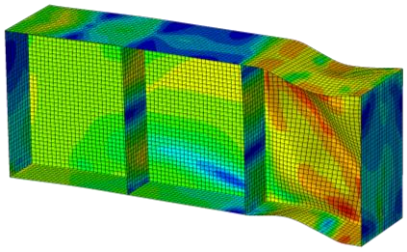

Fig. 8 Failure mode

4. Seismic performance analysis

4.1 Hysteresis curve

The hysteretic curve of the specimen is obtained using the above finite element analysis method, as shown in Figure.9. The analysis results show that each eccentrically braced frame model is at 6Δ. When the forward load reaches the maximum value, The failure mode is that the forward load drops below 85% of the maximum forward value, reaching the failure condition. However, although the BEF-60 meets the destruction conditions, at 4Δ, The brace began to buckle locally. Then the brace's buckling gradually intensified without damaging its energy dissipation beam segment. Comparative analysis of BEF-80, BEF-100, and BEF-125 shows that the hysteretic curve is relatively plump, and the maximum values of positive and negative loads are consistent. Shear failure occurs in all energy-dissipating beam segments. Compared with the hysteretic curve of the frame after replacing the brace, there is no significant decrease in the hysteretic performance.

Comparing the five centrally braced frame models with each other, it was found that with the decrease in

the slenderness ratio of the brace, the area of the hysteretic curve gradually increased, and the shapes were all shuttle-shaped, relatively plump, showing good energy dissipation capacity. Among them, CBF-40 has the smallest hysteretic area and the worst hysteretic performance due to premature out-of-plane instability of the brace; Compared with CBF-60, CBF-70, CBF-80, and CBF-100, it is found that the hysteretic performance gradually increases, and its positive and negative yield capacity, ultimate bearing capacity, and brace failure displacement gradually increase.

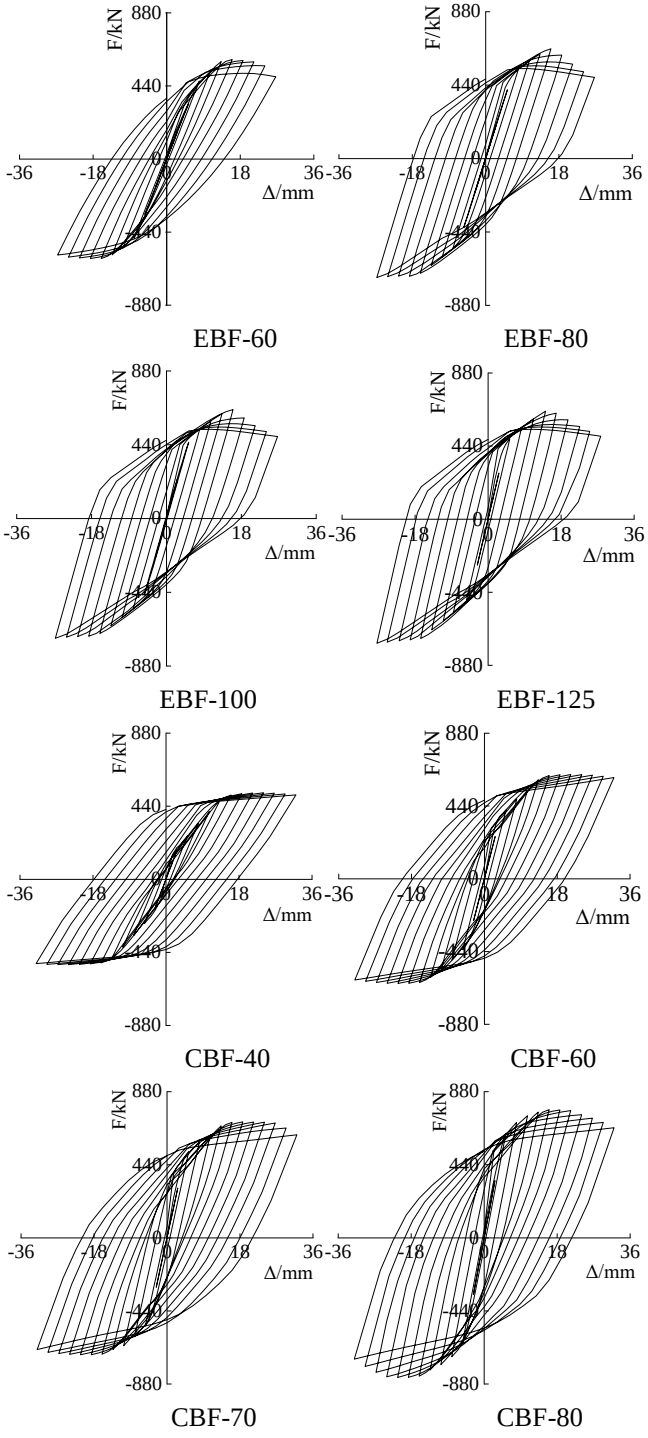

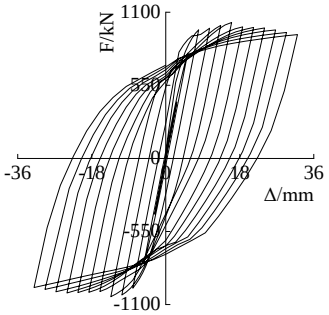

CBF-100

Fig. 9 Hysteresis curve of each mode

4.2 Skeleton curve

The skeleton curve reflects the different stages and characteristics of the component's stress and deformation. From Figure.10(a), it can be seen that in the elastic section, the slope values of the skeleton curves EBF-80, EBF-100, EBF-125, and BASE are the same, all slightly greater than EBF-60; In the same Δ The difference between the positive and negative ultimate bearing capacities is slight, and the displacements corresponding to the maximum bearing capacity of the model are all within 6Δ, The positive and negative bearing capacities of EBF-60 are both smaller than the test bearing capacity, which is due to the large slenderness ratio leading to premature instability of the brace.

Figure.10(b) shows that the skeleton curve has good symmetry in the positive and negative directions. The slope values of the elastic segments of CBF-40, CBF-60, CBF-70, CBF-80, and CBF-100 increase in turn, and the bearing capacity of the specimen exhibits a linear relationship with displacement; As the slenderness ratio of the brace decreases, the displacement corresponding to the maximum bearing capacity of the model gradually advances; In the same Δ, The positive and negative ultimate bearing capacities increase in turn and both decrease, with the CBF-80 bearing capacity decreasing the fastest.

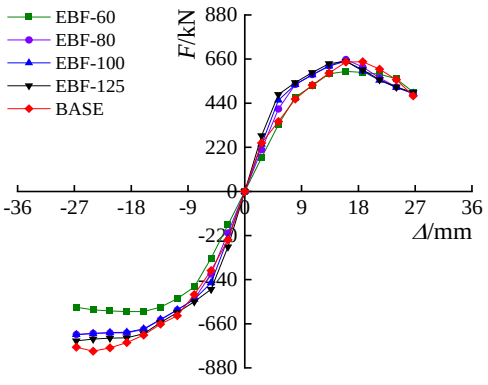

（a）Eccentrically beace frame

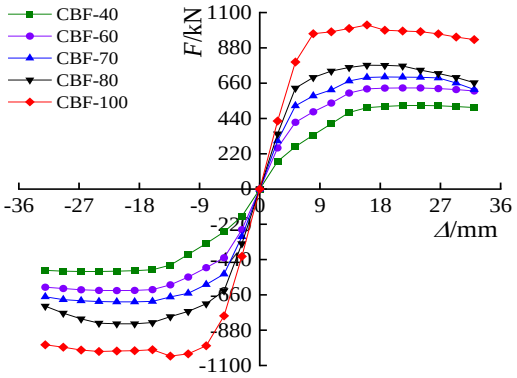

（b）Center brace frame

Fig. 10 Skeleton curve

4.3 Energy consumption

The energy dissipation capacity of the structure is measured by the cumulative energy dissipation W, the energy dissipation coefficient E, and the equivalent viscous damping coefficient h_e. From the analysis in Figure.11, it can be seen that: (1) Eccentric brace and central brace follow the Δ As the level increases, the cumulative energy consumption of each model shows a gradually increasing trend; (2) Eccentric brace is the same as central brace Δ Under the hierarchy, the cumulative energy consumption of models with small slenderness ratios is greater than that of models with large slenderness ratios. (3) In the same Δ Under grade comparison, the energy consumption growth trend of each curve of the eccentric brace in the early stage is relatively uniform. From 6Δ, The growth trend of energy consumption gradually slows down after this stage. At the same time, the EBF-60 has lower energy consumption due to the unstable brace.

The overall growth trend of each curve of the central brace from the 4Δ level is more uniform because the brace provides the main energy dissipation of the frame from this stage. From the analysis of Figure.12, it is found that EBF-60 has the smallest E and h_e coefficients due to the instability of the brace, and the remaining energy dissipation coefficients E and equivalent viscous damping coefficients he is the same for each eccentrically braced model. From this, it can be seen that the Eccentric Braced Frame has no significant change in E, he with the decrease of the brace length to slenderness ratio under the satisfaction of the damage mechanism. The dissipation coefficient E and equivalent viscous damping coefficient he of the centrally braceed frame increase with the decrease of the brace length/slenderness ratio. The dissipation coefficients E of CBF-60, CBF-70, CBF-80, and CBF-100 increase by 2.47%, 5.29%, 9.21%, and 10.40% respectively compared to CBF-40, and the damping coefficients h_e increase by 3.22%, 6.45%, 12.90%, and 16.13% respectively compared to CBF-40.

In general, the energy dissipation capacity of frames with small slenderness ratios of braces is better than that of frames with large slenderness ratios of braces. However, the impact on central braced structures is more obvious.

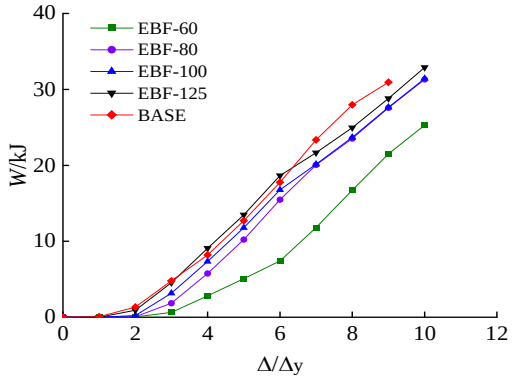

（a）Eccentrically beace frame

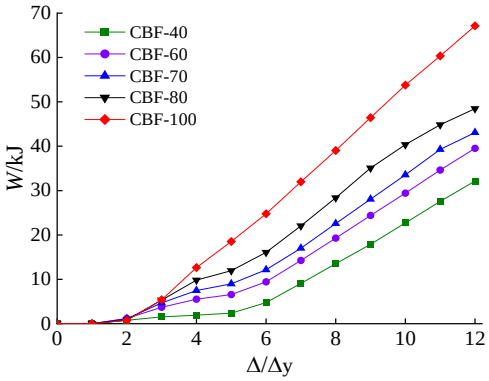

（b）Center brace frame

Fig. 11 Cumulative energy consumption curve

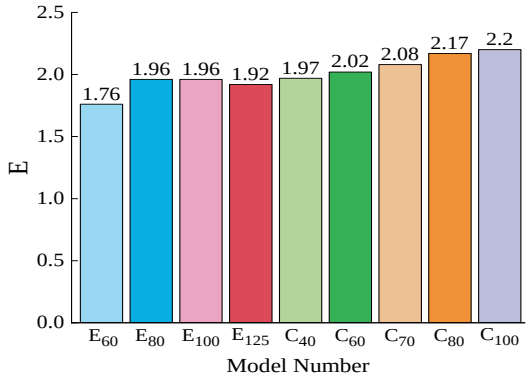

（a）energy dissipation coefficient

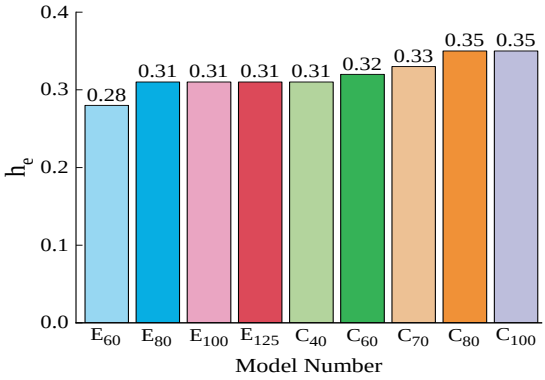

（b）equivalent viscous damping coefficient

Fig. 12 Comparison of energy consumption capacity

4.4 Stiffness analysis

Stiffness degradation reflects how structural stiffness is damaged in resisting earthquakes. In this paper, secant stiffness is used to evaluate the stiffness degradation of the structure, and the lateral stiffness K_i:

$$K_i = \frac{|+F_i| + |-F_i|}{|+\Delta_i| + |-\Delta_i|} \#(1)$$

F_i represents the peak load corresponding to the *i*-level loading point, Δ_i represents the peak displacement corresponding to the *i*-level loading point, and the positive and negative signs represent the loading direction. From Figure.13(a), it can be seen that the stiffness values of each curve are in the top 3Δ. The significant difference indicates that the smaller the slenderness ratio of the brace, the greater the initial stiffness of the frame. Except for the out-of-plane instability of the EBF-60 brace, other models gradually tend to follow a curve with the increase of the loading level but still have stiffness when the component fails. As shown in Table. 5, the minimum initial stiffness value of EBF-60 is 62.9kN/mm, the failure stiffness value is 20.10kN/mm, and the maximum initial stiffness value of EBF-125 is 103.89kN/mm, the failure stiffness value is 23.17kN/mm, which is 39.46% higher than the initial stiffness value. However, the EBF-125 stiffness degradation rate is faster. In the failure state, EBF-60 decreases to 31.96% of the initial stiffness, and EBF-125 decreases to 22.30%. It can be seen that the difference in the slenderness ratio of the brace has a significant impact on the initial stiffness and early stiffness degradation rate of the eccentric brace.

Figure.13(b) shows that the stiffness degradation curves of the five specimens do not exhibit significant abrupt changes, and the degradation trend is relatively uniform. The smaller the slenderness ratio of the brace, the greater its initial stiffness, and conversely, the faster the stiffness degradation rate Δ It is obvious. However, the component still has stiffness when it is damaged. The stiffness degradation curve of the specimen with a small brace slenderness ratio is always higher than that of the specimen with an extensive brace slenderness ratio, but with Δ. The curve tends to flatten with the increase, and the gap gradually decreases. From Table.5, it can be seen that the slenderness ratios of the five central braces decreased by 33.3%, 14.2%, 12.4%, and 20.1% in turn, and the initial stiffness values of the structure increased by 32.7%, 14.8%, 12.6%, and 19.0% in turn, in an inverse relationship. The degree of stiffness degradation was 75.29%, 79.96%, 81.98%, 83.04%, and 81.20%, respectively. The decrease in stiffness degradation of CBF-100 is mainly due to the minimal slenderness ratio of the brace, which leads to excessive brace strength, premature local buckling at the column base, and poor brace performance.

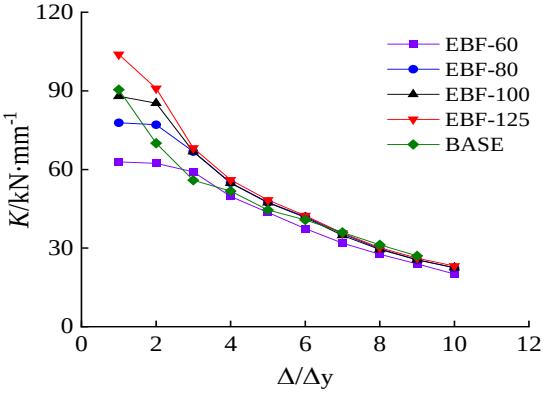

（a）Eccentrically beace frame

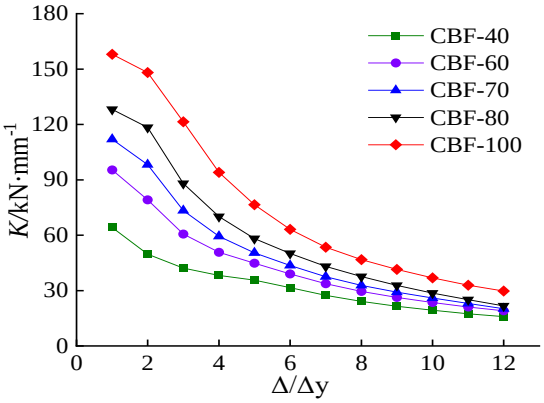

（b）Center brace frame

Fig. 13 Stiffness degradation

Tab. 5 Material properties of steel

Model	initial stiffness	residual stiffness	ratio of residual stiffness
EBF-60	62.90	20.10	31.96
EBF-80	77.82	22.46	28.86
EBF-100	87.95	22.53	25.62
EBF-125	103.89	23.17	22.30
BASE	90.49	27.00	29.84
CBF-40	64.14	15.85	24.71
CBF-60	95.33	19.10	20.04
CBF-70	111.92	20.17	18.02
CBF-80	128.16	21.73	16.96
CBF-100	157.96	29.70	18.80

4.5 Ductility

Ductility reflects whether a structure has sufficient plastic deformation to dissipate seismic energy. In this paper, the "equivalent elastic stiffness method" is used to determine the yield displacement of the frame Δy and yield load Fy; The displacement when the load decreases to 85% of the peak load is the ultimate displacement Δu. The displacement ductility coefficient of its frame is:

$$\mu = \frac{\Delta_u}{\Delta_y} \#(2)$$

Table.7 shows that as the slenderness ratio of the brace decreases, the yield displacement of the eccentric brace Δy gradually decreases, with a sequential difference of about 11% for each model. EBF-60's Δy max, EBF-125's Δy is the smallest, while the displacement ductility coefficient gradually increases from 0.4~0.6, enhancing the structural deformation performance gradually. The yield load, Fy, of models EBF-80, EBF-100, and EBF-125 gradually decreased by about 3.8%, while the main reason for the minimal yield load Fy of EBF-60 was the instability failure of the brace.

The yield displacement Δy of the five central brace frames decreases first and then increases. The Δy of CBF-40 is the largest, and the Δy of CBF-80 is the smallest, with a difference of 25.8%.The yield load Fy gradually increases when λ< 61.61, Fy increased significantly, with the most significant difference between CBF-80 and CBF-100, at 29.4%. When λ> 100, that is, the Fy of the CBF-40 drops to a minimum of 64.3% of the maximum value. Mainly because: when λ≥100, the central brace rod belongs to a large flexibility rod, and

the intermediate region of the brace is prone to out-of-plane instability damage (Fig.14(a)); When 61.61<λ<100, the central brace rod belongs to a medium flexibility rod, and the entire brace has a failure phenomenon of central region section buckling and both ends section depression, without significant instability (Fig.14(b)); When λ≤61.61, the central brace rod belongs to a small flexibility rod, resulting in excessive rigidity of the brace, causing severe distortion of the brace at the node plate connection, warping of the beam-column flange, and bulging of the beam-column web (Fig.14(c)).

From the perspective of the failure phenomenon, the brace stiffness gradually increases with the decrease in slenderness ratio, resulting in a decrease in yield displacement, an increase in yield load, and an increase in displacement ductility coefficient. The yield displacement of CBF-100 increases, and the displacement ductility coefficient decreases, mainly because the brace is too strong and rigid, damaging the beam and column.

Tab. 6 Material properties of steel

Model	Δ_y/mm	Δ_u/mm	F_y/kN	F_u/kN	μ
EBF-60	9.48	21.36	493.59	598.58	2.25
EBF-80	8.42	24.03	541.35	657.60	2.85
EBF-100	7.37	24.03	521.54	649.83	3.26
EBF-125	6.22	24.03	506.62	648.14	3.86
CBF-40	8.08	16.08	323.91	518.55	1.99
CBF-60	6.58	18.76	439.40	611.53	2.85
CBF-70	6.21	24.12	530.08	620.55	3.88
CBF-80	5.99	26.80	640.63	662.56	4.47
CBF-100	6.45	32.04	906.49	931.38	4.97

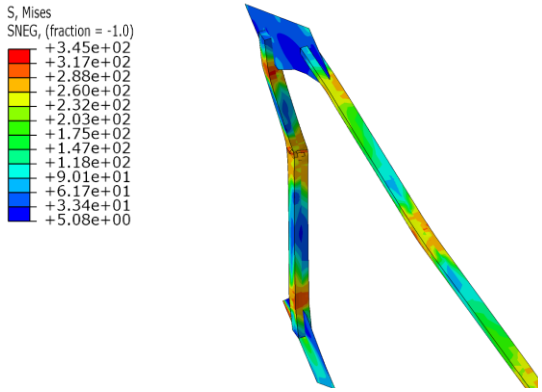

Fig.14(a) CBF-40

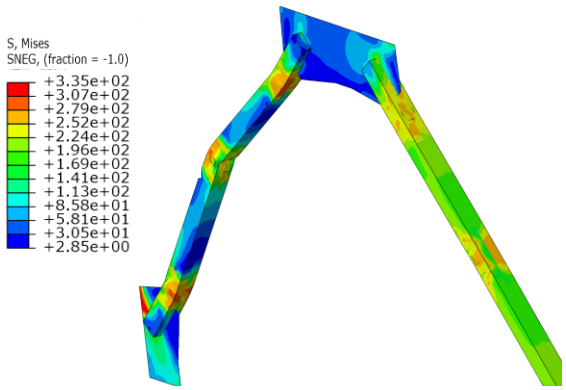

Fig.14(b) CBF-80

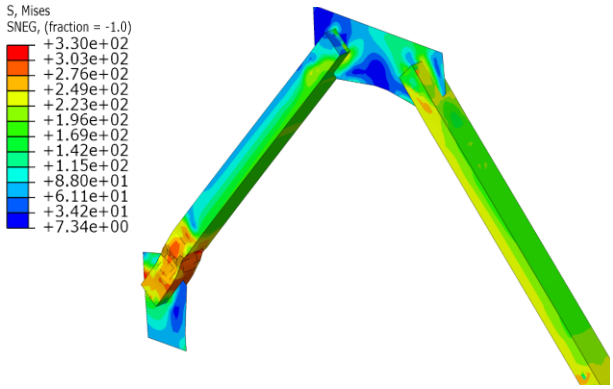

Fig.14(c) CBF-100

Fig. 14 Failure modes of braces with different slenderness ratios

5. Conclusion

Based on experiments, this paper compares the impact of the slenderness ratio of braces on the seismic performance of different frame brace structure systems through nonlinear numerical simulation and obtains the following conclusions:

1) The numerical results are in good agreement with the experimental results, indicating the reliability of using numerical simulation to analyze the structure's seismic performance.
2) Compared to eccentrically braced structures, the change in slenderness ratio has a more significant impact on the seismic resistance of centrally braced structures.
3) For eccentrically braced structures, excessive slenderness ratios can lead to weaker brace stability and subsequent instability of the brace. The energy dissipation beam segment does not exhibit damage, which is not consistent with its failure mechanism; The gradual decrease in slenderness ratio mainly improves the ductility and initial stiffness of the structure but will accelerate the degradation rate of the initial stiffness of the structure.
4) With the brace's slenderness ratio decrease, the hysteretic performance, ultimate bearing capacity, energy dissipation, initial stiffness, and ductility of the centrally braceed structural system will increase. However, if the slenderness ratio is too small, the brace will be too strong to cause the beam and column to fail first, which is not consistent with its failure mechanism; The decrease rate of the slenderness ratio is proportional to the increase rate of initial stiffness of the structure in a 1:1 ratio, which will lead to a significantly faster rate of stiffness degradation in the early stage; Considering the material properties, failure modes, and seismic performance of the structure, it recommended to take $61.61<\lambda<100$。

References

[1] LOU Yu, WEN Lingyan, LI We, et al. Experimental study on seismic performance of steel frame-K shaped brace structure system [J]. Joumal of Building Structues, 2022, 43 (11): 32-40.
[2] YANG Junfen, GU Qiang, WAN Hong, et al. Research on pushover test of inverted-V concentrically braced steel fram [J]. Xi'an Univ. of Arch. & Tech (Natural Science Edition), 2010, 42(05): 656-662.
[3] SUN Yuezhou. Static and dynamic analyses of dual systems of concentrically chevron braced frames [D]. Harbin Institute of Technology, 2006.
[4] CUI Yao, ZHANG Wei, WANG Xin, et al. The Influence of Beam-to-Column Connection Details on the Seismic Performance of Concentrically Braced Frames [J]. Progress in Steel Building Structures, 2021, 23 (04): 1-8.
[5] Tremblay R, Archambault M H, Filiatrault A. Seismic Response of Concentrically Braced Steel Frames Made with Rectangular Hollow Bracing Members [J]. Journal of Structural Engineering. 2003, 129(12): 1626-1636.
[6] Habib G, Jouneghani AH. Experiment al study on hysteretic behavior of steel moment frame equipped with elliptical brace [J]. Steel and Composite Structures, 2020, 34(6).
[7] Mohammed DR, Ismael MA. Effect of Semi-rigid Connection on Post-buckling Behavior of Braced-Steel Frames [M].Springer International Publishing,2019:547-556
[8] Rai DC, Goel SC. Seismic evaluation and upgrading of chevron braced frames [J]. Journal of Construction al Steel Research, 2003, 59(8): 971-994.
[9] Lai JW, Mahin SA. Experimental and analytical studies on the seismic behavior of conventional and hybrid braced frames, PEER Report 2013/20[J]. University of California, Berkeley, 2013.
[10] Yang TY, Moehle JP, Stojadinović B. Performance evaluation of innovative steel braced frames [M]. Pacific Engineering Research Center, College of Engineering, University of California, Berkeley, 2009.
[11] American Institute of Steel Construction. Seismic Provisions for Structural Steel Buildings: ANSI/AISC341-16[S]. Chicago: American Institute of Steel Construction, 2016.
[12] SUN Qing. Research on seismic performance of steel frame structure based on different brace [D]. Qingdao University of Technology, 2021.
[13] ZHAO Kun.Study on Seismic Behavior of High Strength Steel Composite Y-eccentrically Braced Steel Frames on Remote Collaborative Hybrid Test [D]. Xian: Xian University of Architecture and Technology, 2021.
[14] WU KaiDi. Hysteretic energy analysis of concentrically and eccentrically braced steel frames under rare earthquakes [D].Suzhou University of Science and Technology, 2021.
[15] YANG Rongqian, ZHOU Xuejun. Low-Cyclic Reversed Loading Tests of Chevron Concentrically Braced Steel Frames with Semi-Rigid Connections of Different Details [J]. Progress in Steel Building Structures, 2021, 23(12):75-84.
[16] Ministry of Housing and Urban-Rural Development of the People's Republic of China. Technical Specification for Steel Structure of Tall Building: JGJ 99-2015[S]. Beijing: China Architecture & Building Press, 2015.
[17] Ministry of Housing and Urban-Rural Development of the People's Republic of China. Code for Seismic Design of Buildings; GB50011-2010[S]. Beijing: China Architecture & Building Press,2010
[18] MEN YiAng. Research on the pseudo static test of the K-type eccentric braced steel frame[D].He nan. Henan Polytechnic University, 2020.
[19] Ministry of Housing and Urban-Rural Development of the People's Republic of China. Specification for seismic test of buildings.JGJ/T101-2015[S]. Beijing: China Architecture & Building Press,2015
[20] State General Administration of the People's Republic of China for Quality Supervision and Inspection and Quarantine. Metallic materials-Tensile testing-Part 1: Method of test at room temperature. GB/T228.1-2010[S].Beijing: Standards Press of China,2011